γ-Ray Beams with Large Orbital Angular Momentum via Nonlinear Compton Scattering with Radiation Reaction

Yue-Yue Chen,[1,*] Jian-Xing Li,[1,2] Karen Z. Hatsagortsyan,[1,†] and Christoph H. Keitel[1]
[1]*Max-Planck-Institut für Kernphysik, Saupfercheckweg 1, 69117 Heidelberg, Germany*
[2]*School of Science, Xi'an Jiaotong University, Xi'an 710049, China*

(Received 13 February 2018; published 13 August 2018)

Gamma-ray beams with a large angular momentum may affect astrophysical phenomena, which calls for appropriate earth-based experimental investigations. For this purpose, we investigate the generation of well-collimated γ-ray beams with a very large orbital angular momentum using nonlinear Compton scattering of a strong laser pulse of twisted photons at ultrarelativistic electrons. Angular momentum conservation among absorbed laser photons, quantum radiation, and electrons is numerically demonstrated in the quantum radiation-dominated regime. We point out that the angular momentum of the absorbed laser photons is not solely transferred to the emitted γ photons, but due to radiation reaction shared between the γ photons and interacting electrons. The efficiency of the angular momentum transfer is optimized with respect to the laser and electron beam parameters. The accompanying process of electron-positron pair production is furthermore shown to enhance the orbital angular momentum gained by the γ-ray beam.

DOI: 10.1103/PhysRevLett.121.074801

Vortex light is an electromagnetic field that carries orbital angular momentum (OAM). It has a spiral phase ramp around a singularity and a Poynting vector resembling a corkscrew, rotating about the propagation axis [1]. Recently, very promising concepts were developed to upgrade near-IR vortex beams to very high intensities [2–4]. Meanwhile, generating γ rays by Compton scattering with intense laser pulses has been demonstrated in recent experiments [5–8]. Both developments combined together provide a possibility to generate γ-ray beams with very high OAM using nonlinear Compton or Thomoson scattering of twisted light off ultrarelativistic electrons.

In the ultraintense regime $\xi \gg 1$, the coherence length of the photon emission in the nonlinear Compton process is ξ times less than the laser period T. As a consequence, the electron during the emission of the γ photon experiences the laser field as an almost constant field, rather than the structure of the laser field that carries the information on the OAM. Therefore, the emitted single γ photon in the ultraintense regime is not twisted, i.e., not in a certain angular momentum state. However, since the electromagnetic fields of twisted light have spatial symmetry, different electrons in the beam emit spatially correlated γ photons, which results in collective OAM. Thus, the beam of incoherent γ photons produced via the laser scattering by a beam of electrons possess OAM with respect to the propagation axis.

Gamma-ray beams with a total OAM could impact the dynamics of rotating astrophysical objects. These kinds of γ-ray beams are conceivable in an astrophysical environment [9–13]. For example, the radiation from an accretion disk around a Kerr black hole experiences a well-defined phase variation and polarization rotation due to gravitational effects and therefore has both spin and OAM [9]. Another example is connected with radiation emitted by luminous pulsars [14] and quasars, which propagate through inhomogeneous surroundings, experiencing behavior analogous to light propagating through a spiral phase plate [15]. The acquired OAM of radiation can be transferred to the incoherent γ-ray beam by nonlinear inverse Compton scattering in the corona of black holes, magnetosphere, and nebula of pulsars [12]. When the OAM of γ-ray beams is absorbed by a nearby astrophysical object, for example, by the magnetosphere of the companion star in a binary star system, an extra rotation can be imprinted on it, modifying the dynamics. For a simulation of this type of phenomena in laboratory astrophysics, γ-ray beams with a large OAM are required.

The emitted photons due to Compton scattering of the vortex laser beam by an electron will be twisted if during the photon formation the electron experiences the vortex structure of the laser field. This will be the case if the electron can be represented as a plane wave and the photon formation length is comparable with the laser wavelength. The latter takes place when the laser field parameter is not large, $\xi \equiv eE_0/(mc\omega_0) \lesssim 1$ [16], where E_0 and ω_0 are the laser field amplitude and the frequency, respectively, $-e$ and m are the electron charge and mass, respectively, and c is the speed of light. The perturbative regime of Compton scattering, $\xi \ll 1$, when one laser twisted photon is scattered off an ultrarelativistic electron into a twisted γ photon, with a topological charge similar to the incoming laser field is considered in [17–19]. The topological charge of the emitted twisted γ photons can be increased using

multiphoton phenomena in stronger laser fields. In the classical regime x and γ rays with OAM have been investigated theoretically by Thomoson scattering of laser pulses with either orbital or spin angular momentum (SAM) at a moderate nonlinearity with $\xi \sim 1$ [20,21]. In stronger laser fields with $\xi \gg 1$ [4,22], not only the number of scattered photons, but also the nonlinearity, is dramatically increased, which may enhance significantly the OAM of the emitted photon beam. Using the interaction of intense twisted lasers with plasma, γ rays with a large OAM are envisaged [23–25]. However, the twisted γ-photon emission is not highly energetic in [23] and not collimated in [25].

In this Letter, we investigate the production of γ-ray beams with a large OAM by Compton scattering of an intense laser beam of twisted photons by ultrarelativistic electrons in the quantum radiation-dominated regime (QRDR) (see Fig. 1), i.e., when the radiation energy during a laser period is comparable with the electron energy. To this end, the angular momentum evolution of the quantum radiation is calculated numerically with a semiclassical method, where the electron dynamics in the laser field is calculated classically and the photon emission and possible further pair production via quantum electrodynamics with the Monte Carlo algorithm in [26–28]. As a key result, a high energy γ-photon beam with both very high OAM and collimation is generated. In contrast to previous works [17–21,29], we further demonstrate that, when the radiation reaction is accounted for, part of the OAM and SAM of the absorbed laser photons is transferred to the electron beam. Moreover, the accompanying pair production process is shown to cause a counterintuitive increase of the OAM of the γ beam due to extra absorption of twisted laser photons by secondary particles.

We consider interaction of an intense Laguerre-Gaussian (LG) laser pulse (circularly or linearly polarized) with a counterpropagating ultrarelativistic electron beam. Each photon of a $\mathrm{LG}_{p\ell}$ beam carries $\hbar\sigma_z$ of SAM and $\hbar\ell$ of OAM [1,30], where ℓ is the topological charge. The interaction is in the QRDR [16] when $\alpha\xi\chi \gtrsim 1$ and the quantum nonlinearity parameter $\chi \gtrsim 1$, with fine structure constant α, $\chi \approx 2(\omega_0/m)\xi\gamma$, and the electron Lorentz factor γ. The generated γ-ray beam with OAM is well collimated in the regime $\gamma \gg \xi$, with the emission angle $\theta \sim \xi/\gamma$ [16]. The laser beam is described by a paraxial solution [31,32] and parameters are chosen as $\xi = 120$, $\lambda_0 = 1$ μm, $\chi \approx 4$, $\ell = 1$, $w_0 = 2\lambda_0$, and $\omega_0\tau_p/2\pi = 6$. The electron beam, with a length of λ_0 and a radius of $4\lambda_0$, consists of 2×10^5 electrons with initial energy $\gamma = 10^4$ and has a transverse spatial Gaussian distribution with a width of $\sigma_\perp = 1.2\lambda_0$.

The total emission energy in the case of a linearly polarized LG mode is shown in Fig. 1. The energy distribution of the γ-ray beam has a ring-shaped intensity profile, indicating that it carries OAM. The quantitative evaluation of OAM is presented in Fig. 2 for two cases: a LG laser pulse with circular polarization and a circularly polarized Gaussian laser field with $\sigma_z = 1$ (the results of a linearly polarized LG laser pulse are presented in the Supplemental Material [31]). The OAM of γ photons, electrons, and positrons with respect to the z axis are calculated with $L_z = xp_y - yp_x$, where p_x and p_y are the components of the linear momenta, and x and y are the coordinates of the particles (for the γ photon it is the emission coordinate, as the formation length of the photon is well localized in this ultrarelativistic regime). The total

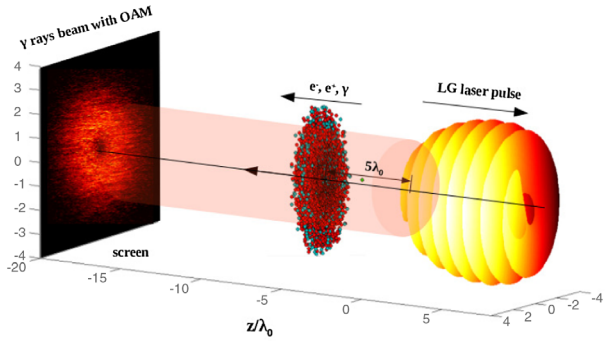

FIG. 1. Scheme for generation of a γ-ray beam with OAM. An intense Laguerre-Gaussian laser beam of linear (illustrated in the figure) or circular polarization counterpropagates with and scatters off an electron beam. Electrons absorb multiple laser photons generating a γ photon. The spin and OAM of laser photons are transferred to the electrons and in this way to the γ-photon beam. The radiation energy distribution is illustrated on the screen.

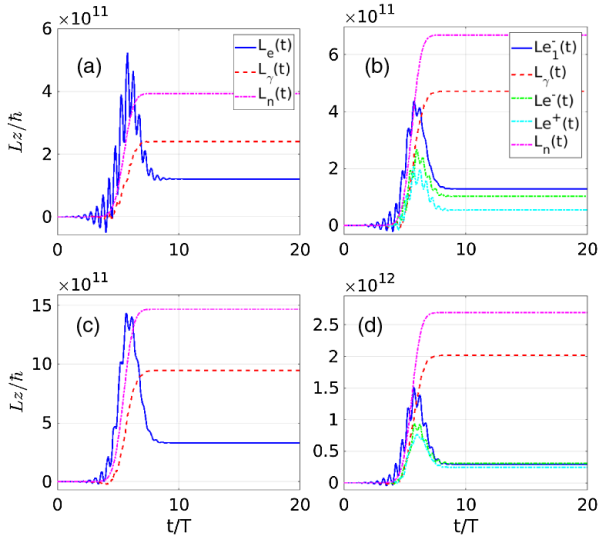

FIG. 2. Angular momentum of γ photons (red dashed), electrons (blue solid), and the absorbed laser photons (magenta dash-dotted) in the (a),(b) circularly polarized Gaussian and (c),(d) LG_{01} laser fields, with accounting for the pair production (right column) and without (left column). The OAM of the created electrons and positrons are shown by green dash-dotted and light blue dash-dotted lines, respectively. The laser and electron parameters are $\xi = 120$ and $\gamma = 10^4$.

angular momentum absorbed from the laser is $L_n = (\ell + \sigma_z)n\hbar$, where n is the number of the absorbed laser photons. The latter is calculated from the energy-momentum conservation $q + nk = q' + k'$, where q, q', and k' are the 4-quasimomenta of incoming and outgoing electrons and the emitted γ photon, respectively. The electron's quasimomenta are estimated via their relationship to the instantaneous electron momentum (see Supplemental Material [33]).

We analyze the evolution of angular momentum described in Fig. 2. In all cases, the angular momentum conservation is fulfilled to good accuracy $(\ell + \sigma_z)n\hbar \approx L_e + L_\gamma$, with the total OAM of the final electrons L_e and that of the γ photons L_γ. Here, the initial OAM of the electron beam vanishes; in the case with the pair production, L_e includes also the OAM of the created electrons and positrons. The total number of absorbed laser photons due to the γ-photon emission is calculated from energy conservation [33]; see the summary in Table I. The contribution of SAM of electrons and positrons L_σ in the angular momentum conservation is negligible and, therefore, is not included. In fact, for the parameters of Table I, L_σ is at most $L_\sigma = N_{e^-e^+}\hbar \sim 10^5\hbar$, which is much smaller than $L_e + L_\gamma \sim 10^{12}\hbar$. In QRDR, the absorbed OAM of the laser photons L_n is not fully transferred to the emitted photon beam but shared between the electrons and the emitted photons. The OAM share of the γ-ray beam is $L_\gamma/(L_e + L_\gamma) \sim 70\%$. This is in contrast to the idealized case of the electron interacting with a moderately strong laser field [34], when $(\ell + \sigma_z)n\hbar = L_\gamma$ is fulfilled. The sign of radiation OAM is determined by both the laser and electrons' angular momenta, contrary to the case of linearly polarized LG at $\xi \sim 1$, where it is opposite of the OAM absorbed laser photons [20].

One should underline that the transfer of OAM is determined by the total number of absorbed laser photons during γ-photon emission, but not with the total energy absorbed from the laser field during the interaction. In fact, a part of the energy absorbed from the laser during photon emission is returned to the laser pulse after the turn-off of the laser field [35]. This ponderomotive energy transfer is not accompanied with an angular momentum transfer. The total energy absorbed from the laser field during the interaction in terms of the photon number $\tilde{n}$ can be evaluated from the energy-momentum conservation involving the electron 4-momenta before and after the interaction p and p', respectively: $p + \tilde{n}k = p' + k'$. The energy difference corresponding to turn-on and turn-off is $\Delta n = n - \tilde{n} = (\xi^2/2)[(1/p' \cdot k) - (1/p \cdot k)]$, which is responsible for upshifting of laser frequency [35]. As confirmed by Table I, the energy conservation is fulfilled by the total number of absorbed laser photons during the interaction $\tilde{n}$. Here, the OAM transfer is determined by the number of the absorbed laser photons n due to γ-photon emission.

A comparison of the cases of different laser fields in Fig. 2 (see also the Supplemental Material [31]) shows that a circular LG_{01} mode is more favorable for generation of a γ-ray beam with a large OAM. For a linear polarized LG_{01} beam, the transverse electric field oscillates along the x direction, resulting in an oscillating OAM $L_z \approx -\sum_i y_i p_{xi}$, as shown in [31]. However, the final OAM for linear LG_{01} mode is much less than that for circular polarization. This is because the absorbed photon number $n(t) \propto a(t)^2$ [33] and circular polarization provides a more steady and larger absorption of twisted photons. Further, due to the spatial structure, the circular LG_{01} mode has three times larger energy than the circular Gaussian mode for the same ξ, and $\hbar$ more OAM in addition to $\hbar$SAM per photon, which results in larger OAM transfer (see Table I).

For the chosen parameters $\xi = 120$ and $\gamma = 10^4$, the quantum parameter is rather large, $\chi \approx 4$, and the pair production effect is not negligible. Our results in Fig. 2 demonstrate the counterintuitive role of pair production. Even though the energy of the γ beam decreases due to pair production, the OAM of radiation shows an unexpected growth. For example, in the case of circular LG_{01}, the total OAM of the γ beam grows up from $9.46 \times 10^{11}\hbar$ to $2.02 \times 10^{12}\hbar$ (see Table I).

To explain the changes of the OAM induced by pair production, energy and OAM spectra in the case of circular LG_{01} are shown in Fig. 3. It can be seen from Fig. 3(a) that a well-collimated γ-ray beam is generated with a spreading angle $\theta < 0.05$ rad (90% of the γ-photon energy is concentrated within this angle). Pair production causes a depletion of hard photons in region I, while emission of pairs contribute to an increase of low energy photons in region II, as shown in Fig. 3(b), because the created electrons and positrons have lower energies, lower χ values, and emit lower energy photons. Because of the lower energy, the created electrons and positrons oscillate within

TABLE I. OAM (in units of $\hbar$) and energy changes (in units of mc^2) of electrons and photons after the interaction, according to Fig. 2. Left and right subcolumns correspond to without and with pair production, respectively. Subscripts e and γ denote charged particles and emitted photons, respectively, n is the number of absorbed laser photons due to the γ-photon emission, $\tilde{n} \equiv \Delta E_e + E_\gamma/\hbar\omega_0$ is the laser energy change described by a photon number, N_γ is the γ-photon number, and $\bar{\ell}$ is the average topological number.

	Circular Gaussian		Circular LG_{01}	
$L_e + L_\gamma$	3.61×10^{11}	7.57×10^{11}	1.28×10^{12}	2.86×10^{12}
L_γ	2.4×10^{11}	4.72×10^{11}	9.46×10^{11}	2.02×10^{12}
$\Delta E_e + E_\gamma$	5.31×10^5	1.06×10^6	1.02×10^6	2.25×10^6
E_γ	1.65×10^9	1.54×10^9	1.8×10^9	1.67×10^9
n	3.93×10^{11}	6.69×10^{11}	7.33×10^{11}	1.35×10^{12}
$\tilde{n}$	2.19×10^{11}	4.38×10^{11}	4.21×10^{11}	9.29×10^{11}
N_γ	3.51×10^6	4.86×10^6	4.29×10^6	6.69×10^6
$\bar{\ell}$	6.74×10^4	9.6×10^4	2.19×10^5	2.99×10^5

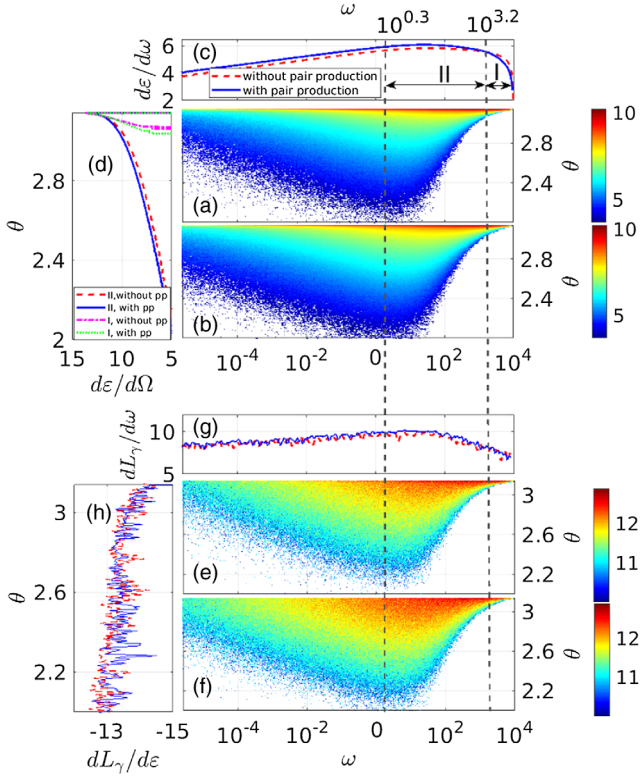

FIG. 3. Radiation energy $\log_{10}[d\varepsilon/d\omega/d\Omega]$ rad^{-1} (a),(b) and OAM $\log_{10}[dL_\gamma/d\Omega/d\omega]$ (e),(f) distributions for circular LG_{01} mode, without (a),(e) and with pair production (pp) (b),(f). (c) Radiation spectral distribution with (blue solid lines) and without (red dashed lines) pair production. (d) Angular distribution of radiation in regions I ($\omega > 10^{3.2}$) and II ($10^{0.3} < \omega < 10^{3.2}$). (g) OAM vs photon energy, and (h) OAM per radiation energy $dL/d\varepsilon \equiv (dL_\gamma/d\Omega)/(d\varepsilon/d\Omega)$ vs θ, with (solid blue lines) and without pair production (red dashed lines) $\xi = 120$, $\gamma = 10^4$, OAM is in units of $\hbar$, and energies in units of mc^2.

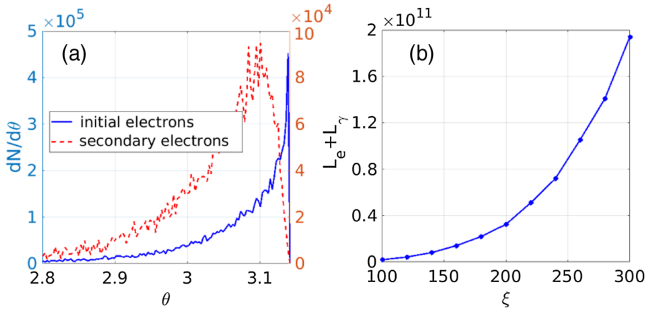

FIG. 4. (a) Angular distribution of initial electrons (solid) and secondary electron and positrons (dashed). (b) Total OAM vs ξ, with $\chi = 4$, $N_e = 2 \times 10^4$.

a larger angle $\theta \sim \xi/\gamma$ with respect to the axis of the electron beam, as shown in Fig. 4(a), and emit γ photons with larger angular spread; see the increased angular spreading due to pair production in Figs. 3(b) and 3(d). As the OAM per unit power is inversely proportional to θ, as shown in Fig. 3(h), the increase of emission in a large angle by pairs lead to an increase of OAM for region II, as shown in Fig. 3(g). While the increase of OAM in region I is roughly counteracted by photon number depletion. A clear increase of the angular spreading due to pair production in the large OAM regime can be seen in Fig. 3(f). Therefore, the angular redistribution caused by pair production results in the increase of OAM for the total γ beam.

Intense femtosecond vortex light with a few to a hundred millijoule has been experimentally generated at infrared wavelength [2,3]. Meanwhile, amplification of twisted laser intensities by 2 orders of magnitude is shown in plasma with stimulated Raman backscattering [4]. With these advanced techniques and possible further improvement, such as multistaging, petawatt class twisted lasers used in our scheme can be realized in near future. A well-collimated γ-photon beam can then be generated with a brightness of about 6.4×10^{22} photons/s/ mm^2/mrad^2. The average OAM per photon emitted within the angular spread of $\Delta\theta \approx 0.05$ rad is $2.7 \times 10^4\hbar$. Our scheme can produce γ-ray beams with GeV photons, i.e., with photon energy $\sim$10 times higher than the copropagating scheme [23] in a much smaller angular spread ($\sim$10 times smaller than the all-optical scheme [25]).

We point out that the OAM of incoherent radiation in the ultrarelativistic QRDR is the property of the whole beam, rather than the property of single photons. If the initial beam contains $N_e = 2 \times 10^{10}$ electrons, the total OAM of a γ-ray beam within $\theta > \pi - 0.05$ rad is $L_\gamma \approx 1.9 \times 10^{16}\hbar$. The OAM of radiation can be largely increased by using a more intense laser field [see Fig. 4(b)], however, at the expense of its collimation [33].

The collective OAM of a γ beam can have a mechanical impact for dynamics of astrophysical objects. For instance, the γ jets emitted by a pulsar can be absorbed by the magnetosphere of the companion star in a binary system, and if they carry OAM, the absorption could disturb the rotation of the magnetosphere. We may estimate this effect taking into account that the pulsar luminosity at 1 GeV photon energy is around 10^{35} erg s^{-1} [14]. The OAM provided by the γ jet during the interaction time τ can be estimated via the number of photons N_γ as $L_\gamma \sim 2N_\gamma\hbar \sim 10^{38}\tau\hbar$ [31]. Assuming that the γ jet with an opening angle $\theta \sim 10^{-2}$ rad interacts with part of the magnetosphere of its companion star at a distance $d = 10^7$ cm, the interaction region can be regarded as a plasma disk with radius $R \sim d\theta \sim 10^5$ cm. The additional rotation frequency induced by the γ jet with OAM can be estimated as $\Delta\Omega \sim (L_\gamma/\hbar)(r_p^2/R^4)(m_c/m_p)\lambda_c \sim 10^{-12}\tau$ s^{-1}, with the proton radius r_p and the proton mass m_p [31]. The significance of the disturbance of the rotation induced by the γ jet can be evaluated by comparing it with the pulsar's glitch parameters. For instance, the glitch duration of the Crab pulsar is about 10 days ($\sim 10^6$ s) during which the pulsar frequency change is about

$\Delta\Omega_{\mathrm{glitch}} \sim \Omega_{\mathrm{pulsar}} 10^{-8}$–$10^{-6}$ s^{-1} [36]. From our estimate above, we obtain $\Delta\Omega \sim 10^{-6}$ s^{-1} at $\tau \sim 10^{6}$ s; i.e., the disturbance of the rotation induced by the γ jet is comparable to the pulsar's glitch parameters.

Concluding, we showed a possibility for generation of well-collimated γ-ray beams with a large OAM in the ultrarelativistic quantum radiation-dominated regime, employing incoherent Compton scattering of twisted light by an electron beam. In contrast to the low intensity regime, each γ photon is not in a certain OAM state, but the total γ-ray beam carries a large angular momentum with respect to the beam axis. Such beams can have applications in laboratory astrophysics.

*yue-yue.chen@mpi-hd.mpg.de
†k.hatsagortsyan@mpi-hd.mpg.de

[1] L. Allen, M. W. Beijersbergen, R. J. C. Spreeuw, and J. P. Woerdman, Phys. Rev. A **45**, 8185 (1992).
[2] K. Sueda, G. Miyaji, N. Miyanaga, and M. Nakatsuka, Opt. Express **12**, 3548 (2004).
[3] Y.-C. Lin, Y. Nabekawa, and K. Midorikawa, Appl. Phys. B **122**, 280 (2016).
[4] J. Vieira, R. Trines, E. Alves, R. Fonseca, J. Mendonça, R. Bingham, P. Norreys, and L. Silva, Nat. Commun. **7**, 10371 (2016).
[5] S. Chen, N. Powers, I. Ghebregziabher, C. Maharjan, C. Liu, G. Golovin, S. Banerjee, J. Zhang, N. Cunningham, A. Moorti *et al.*, Phys. Rev. Lett. **110**, 155003 (2013).
[6] G. Sarri, D. Corvan, W. Schumaker, J. Cole, A. Di Piazza, H. Ahmed, C. Harvey, C. H. Keitel, K. Krushelnick, S. Mangles *et al.*, Phys. Rev. Lett. **113**, 224801 (2014).
[7] J. Cole, K. Behm, E. Gerstmayr, T. Blackburn, J. Wood, C. Baird, M. J. Duff, C. Harvey, A. Ilderton, A. Joglekar *et al.*, Phys. Rev. X **8**, 011020 (2018).
[8] K. Poder, M. Tamburini, G. Sarri, A. Di Piazza, S. Kuschel, C. D. Baird, K. Behm, S. Bohlen, J. M. Cole, D. J. Corvan *et al.*, Phys. Rev. X **8**, 031004 (2018).
[9] F. Tamburini, B. Thidé, G. Molina-Terriza, and G. Anzolin, Nat. Phys. **7**, 195 (2011).
[10] F. V. Hartemann, A. L. Troha, H. A. Baldis, A. Gupta, A. K. Kerman, E. C. Landahl, N. C. Luhmann Jr., and J. R. Van Meter, Astrophys. J. Suppl. Ser. **127**, 347 (2000).
[11] P. Stewart, Astrophys. Space Sci. **18**, 377 (1972).
[12] J. Arons, Astrophys. J. **177**, 395 (1972).
[13] T. Takiwaki, K. Kotake, and K. Sato, Astrophys. J. **691**, 1360 (2009).
[14] R. Bühler and R. Blandford, Rep. Prog. Phys. **77**, 066901 (2014).
[15] M. Harwit, Astrophys. J. **597**, 1266 (2003).
[16] A. Di Piazza, C. Müller, K. Z. Hatsagortsyan, and C. H. Keitel, Rev. Mod. Phys. **84**, 1177 (2012).
[17] U. D. Jentschura and V. G. Serbo, Phys. Rev. Lett. **106**, 013001 (2011).
[18] U. D. Jentschura and V. G. Serbo, Eur. Phys. J. C **71**, 1571 (2011).
[19] I. P. Ivanov and V. G. Serbo, Phys. Rev. A **84**, 033804 (2011).
[20] V. Petrillo, G. Dattoli, I. Drebot, and F. Nguyen, Phys. Rev. Lett. **117**, 123903 (2016).
[21] Y. Taira, T. Hayakawa, and M. Katoh, Sci. Rep. **7**, 5018 (2017).
[22] C. Danson, D. Hillier, N. Hopps, and D. Neely, High Power Laser Sci. Eng. **3**, e3 (2015).
[23] C. Liu, B. Shen, X. Zhang, Y. Shi, L. Ji, W. Wang, L. Yi, L. Zhang, T. Xu, Z. Pei *et al.*, Phys. Plasmas **23**, 093120 (2016).
[24] J. Vieira, R. M. G. M. Trines, E. P. Alves, R. A. Fonseca, J. T. Mendonça, R. Bingham, P. Norreys, and L. O. Silva, Phys. Rev. Lett. **117**, 265001 (2016).
[25] Z. Gong, R. H. Hu, H. Y. Lu, J. Q. Yu, D. H. Wang, E. G. Fu, C. E. Chen, X. T. He, and X. Q. Yan, Plasma Phys. Controlled Fusion **60**, 044004 (2018).
[26] N. V. Elkina, A. M. Fedotov, I. Y. Kostyukov, M. V. Legkov, N. B. Narozhny, E. N. Nerush, and H. Ruhl, Phys. Rev. ST Accel. Beams **14**, 054401 (2011).
[27] C. P. Ridgers, J. G. Kirk, R. Duclous, T. G. Blackburn, C. S. Brady, K. Bennett, T. D. Arber, and A. R. Bell, J. Comput. Phys. **260**, 273 (2014).
[28] D. G. Green and C. N. Harvey, Comput. Phys. Commun. **192**, 313 (2015).
[29] S. Stock, A. Surzhykov, S. Fritzsche, and D. Seipt, Phys. Rev. A **92**, 013401 (2015).
[30] L. Allen, V. E. Lembessis, and M. Babiker, Phys. Rev. A **53**, R2937 (1996).
[31] See Supplemental Material at http://link.aps.org/supplemental/10.1103/PhysRevLett.121.074801 for the paraxial solutions of Laguerre-Gaussian beams.
[32] A. April, Opt. Lett. **33**, 1392 (2008).
[33] See Supplemental Material at http://link.aps.org/supplemental/10.1103/PhysRevLett.121.074801 for the applied method of calculation of the number of the absorbed laser photons, the regime of a the more intense laser field, estimations on the application, and the description of the twisted laser field.
[34] M. Katoh, M. Fujimoto, H. Kawaguchi, K. Tsuchiya, K. Ohmi, T. Kaneyasu, Y. Taira, M. Hosaka, A. Mochihashi, and Y. Takashima, Phys. Rev. Lett. **118**, 094801 (2017).
[35] T. Kibble, Phys. Rev. **138**, B740 (1965).
[36] T. Wong, D. C. Backer, and A. G. Lyne, Astrophys. J. **548**, 447 (2001).